nature cell biology

DNA processing is not required for ATM-mediated telomere damage response after *TRF2* deletion

Giulia B. Celli[1,2] and Titia de Lange[1,3]

Telomere attrition and other forms of telomere damage can activate the ATM kinase pathway. What generates the DNA damage signal at mammalian chromosome ends or at other double-strand breaks is not known. Telomere dysfunction is often accompanied by disappearance of the 3′ telomeric overhang[1,2], raising the possibility that DNA degradation could generate the structure that signals[2]. Here we address these issues by studying telomere structure after conditional deletion of mouse TRF2, the protective factor at telomeres. Upon removal of TRF2 from *TRF2*$^{Fl-}$ *p53*$^{-/-}$ mouse embryo fibroblasts, a telomere damage response is observed at most chromosome ends. As expected, the telomeres lose the 3′ overhang and are processed by the non-homologous end-joining pathway. Non-homologous end joining of telomeres was abrogated in DNA ligase IV-deficient (*Lig4*$^{-/-}$) cells. Unexpectedly, the telomeres of *TRF2*$^{-/-}$ *Lig4*$^{-/-}$ *p53*$^{-/-}$ cells persisted in a free state without undergoing detectable DNA degradation. Notably, the telomeres retained their 3′ overhangs, but they were recognized as sites of DNA damage, accumulating the DNA damage response factors 53BP1 and γ-H2AX, and activating the ATM kinase. Thus, activation of the ATM kinase pathway at chromosome ends does not require overhang degradation or other overt DNA processing.

TRF2 is a key component of the human telomeric protein complex[1]. TRF2 binds to double-stranded telomeric DNA and has been implicated in the formation of the t-loop structure[3]. Human telomeres undergo acute deprotection when the telomeric protein TRF2 is removed and also become dysfunctional after excessive shortening in the absence of telomerase (reviewed in ref. 3). In both settings, the ATM kinase is activated and chromosome ends become associated with DNA damage response factors such as 53BP1, γ-H2AX, Rif1 and the Mre11 complex[4,5]. Cells also attempt to repair damaged telomeres using the non-homologous end-joining (NHEJ) pathway, generating telomere–telomere fusions and dicentric chromosomes[1,6]. It is not known how telomere damage is sensed. In yeast, telomere dysfunction leads to degradation of the 5′ strand, resulting in excessive 3′ overhangs[7]. This type of DNA processing has been implicated in the Mec1-dependent response to double-strand breaks (DSBs)[8]. However, in mammalian cells it is not known whether or how DSBs are processed, and what the signal for ATM activation is remains a subject for debate[9]. Telomeres represent a unique opportunity to study these issues because they provide molecularly marked sites that can activate the canonical DNA damage response.

To study the DNA damage response at telomeres, we targeted the mouse *TRF2* gene on chromosome 8 (*Terf2*; Mouse Genome Informatics (MGI) number 1195972; referred to hereafter as *TRF2* for clarity). The *TRF2* locus was modified such that exon 1 (containing the translation initiation site) and exon 2 are flanked by *lox*P sites, allowing inactivation of the *TRF2* gene with Cre recombinase (Fig. 1a). Embryonic stem cells carrying the conditional *TRF2* allele (*TRF2*$^{Fl/+}$) and the null allele (*TRF2*$^{-/+}$) were generated and used to establish mouse strains (see Supplementary Information, Fig. S1a). Intercrosses of *TRF2*$^{-/+}$ mice failed to generate *TRF2*$^{-/-}$ offspring (see Supplementary Information, Fig. S1b, c). Embryonic lethality occurred early in development before embryonic day 13.5 (E13.5) and was not rescued by p53 deficiency (data not shown). Lethality at E5–6 occurs in mice that lack either TRF1 or TIN2 (refs 10, 11). TRF1 and TIN2 are both required to stabilize TRF2 at telomeres[12–14], suggesting that the embryonic lethal phenotype of TRF1, TIN2 and TRF2 deficiency will be substantially similar. Because TRF2 deficiency resulted in a rapid growth defect and genome-wide telomere fusions in cultured cells (see below), the events leading to early death of the embryos were not studied in detail.

The cellular consequences of TRF2 deficiency were determined using mouse embryo fibroblasts (MEFs). Transient expression of Cre recombinase from a self-deleting ('hit-and-run') retrovirus resulted in rapid deletion of the *TRF2* gene, and concomitant loss of TRF2 protein was detectable at ~48–72 h post-infection (Fig. 1b). Indirect immunofluorescence and immunoblotting showed absence of TRF2 and its interacting partner Rap1, suggesting that Rap1 depends on TRF2 for its stable expression. By contrast, TRF1 was still detectable in immunoblots and by immunofluorescence and was present at telomeres (Fig. 1c, d; and data not shown), providing a marker for telomeres in cells lacking TRF2. *TRF2* deletion in MEFs that were derived from p53-proficient embryos resulted

[1]Laboratory for Cell Biology and Genetic, The Rockefeller University, 1230 York Avenue, New York, NY 10021, USA. [2]Present address: Skirball Institute of Biomolecular Medicine, NYU School of Medicine, New York, NY 10016, USA.
[3]Correspondence should be addressed to T.d.L. (e-mail: delange@mail.rockefeller.edu)

Published online: 19 June 2005; DOI: 10.1038/ncb1275

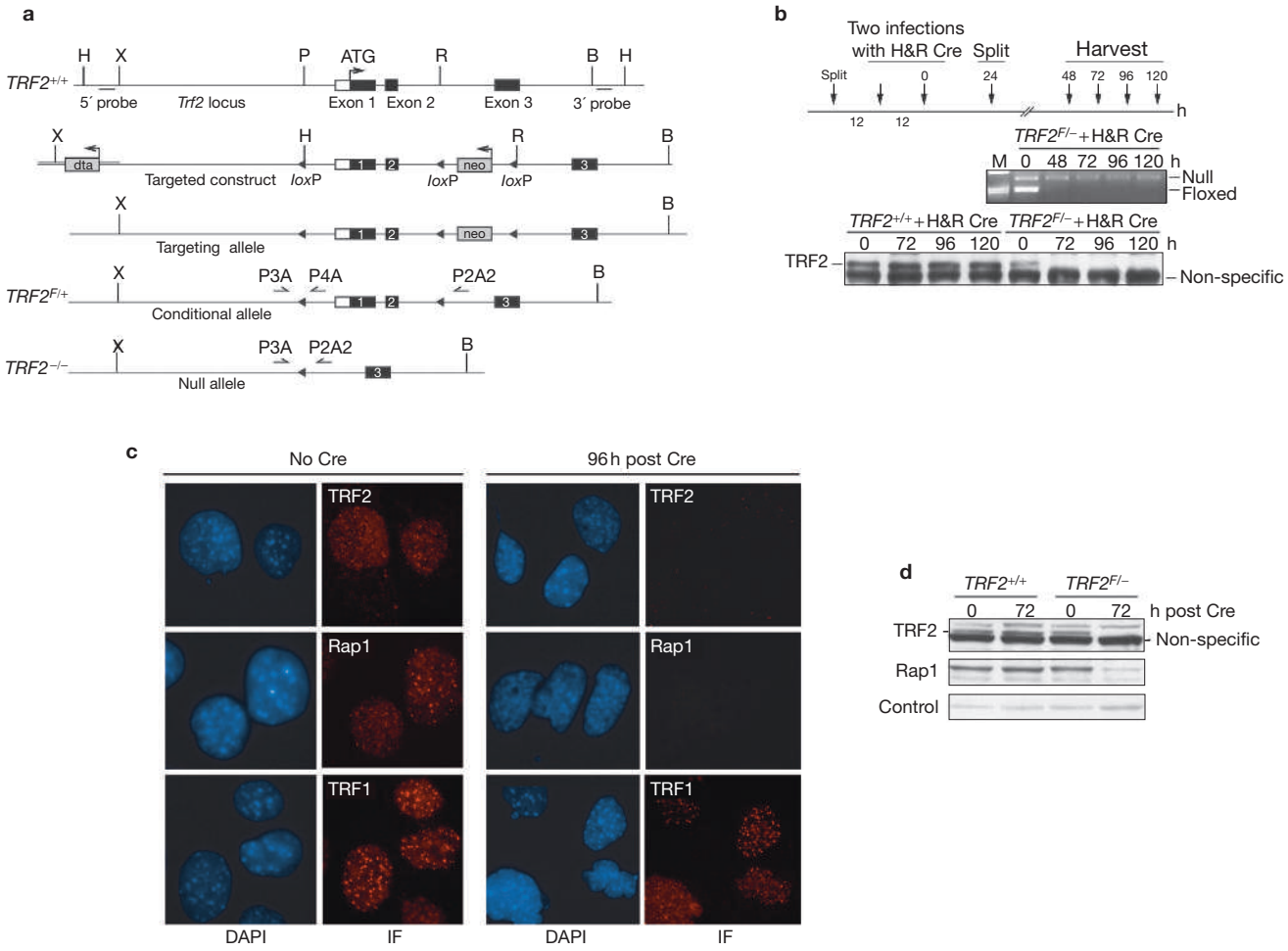

Figure 1 Conditional deletion of mouse *TRF2*. (**a**) Schematic depicting the *TRF2* locus (*TRF2*$^{+/+}$), the targeting construct, the targeted allele, the conditional (*TRF2*$^{F/+}$) allele, and the null (*TRF2*$^{-/-}$) allele. PCR primers used for genotyping are indicated. H, *Hin*dIII; X, *Xho*I; P, *Pst*I; R, *Eco*RI; B, *Bam*HI. (**b**) Top: experimental time line. Middle: PCR analysis with primers P3A, P4A and P2A2 on DNA isolated at the indicated time points. M, molecular weight markers. Bottom: immunoblotting for TRF2 protein at the indicated time points after Cre introduction. (**c**, **d**) Immunofluorescence (IF; **c**) and immunoblot analysis (**d**) to detect TRF2, Rap1 and TRF1 before and 72 or 96 h after introduction of hit-and-run (H&R) Cre into *TRF2*$^{F/-}$ MEFs. MEFs used in **b** and **d** were immortalized by infection with pBabeSV40LT; MEFs in **c** were *p53*-null. Antibodies used in **c** were mTRF1, 644; mTRF2, 1254; mRap1, 1252. Nuclei were counterstained with DAPI. In **b** and **d**, 647 and 765 were used to detect TRF2 and Rap1, respectively.

in a senescence-like arrest (see Supplementary Information, Fig. S1e), prohibiting the analysis of mitotic chromosomes. This arrest was abrogated by p53 deficiency, consistent with previous findings[15–17]. For this reason, the experiments described below were performed with *p53*$^{-/-}$ MEFs.

Deletion of *TRF2* from *TRF2*$^{F/-}$ *p53*$^{-/-}$ MEFs resulted in extensive telomere fusions (Fig. 2). Metaphase spreads obtained 48–96 h after Cre treatment showed a progressive increase in the number of fused telomeres until nearly all telomeres had undergone end joining (Fig. 2a, b). In general, the telomeric signals were retained and were of equal intensity on sister telomeres. Partial loss of telomeric DNA from all chromosome ends was observed sporadically (<1% of metaphases; data not shown) and its significance is not clear. Induction of genome-wide telomere fusions was observed in MEFs from five independent *TRF2*$^{F/-}$ *p53*$^{-/-}$ embryos and also occurred reproducibly in 12 clonal *TRF2*$^{F/-}$ *p53*$^{-/-}$ MEF cell lines (data not shown). The telomere fusion phenotype was rescued when *TRF2*$^{F/-}$ *p53*$^{-/-}$ cells were complemented with a mouse *TRF2* cDNA (see Supplementary Information, Fig. S2), demonstrating that it is caused by TRF2 deficiency.

Although *p53*$^{-/-}$ cells yielded metaphase chromosomes after depletion of TRF2, the cultures eventually perished, presumably due to the inability of the cells to segregate chromosomes in mitosis.

As expected on the basis of previous findings[6], the telomere fusions were largely dependent on DNA ligase IV (encoded by *Lig4*), the ligase that acts together with DNA protein kinase catalytic subunit (DNA-PKcs) and the Ku heterodimer in the NHEJ pathway (Fig. 2b and see Supplementary Information, Table S1). DNA ligase IV-deficient *TRF2*$^{F/-}$ *p53*$^{-/-}$ MEFs were derived from crosses with *Lig4*$^{-/-}$ *p53*$^{-/-}$ mice. *Lig4* status did not affect the deletion of *TRF2* by Cre recombinase (data not shown). After introduction of Cre, *TRF2*$^{F/-}$ *Lig4*$^{-/-}$ *p53*$^{-/-}$ cells showed, on average, 0.5 fusions per metaphase, representing a 120-fold reduction compared with *Lig4*$^{+/+}$ cells (see Supplementary Information, Table S1). In genomic blots, the telomere fusions were evident from the progressive increase in size of telomeric restriction fragments after Cre expression in NHEJ-proficient *TRF2*$^{-/-}$ MEFs (Fig. 3a). In contrast, the telomeric pattern persisted unaltered over 120 h in Cre-treated *TRF2*$^{F/-}$ *Lig4*$^{-/-}$ *p53*$^{-/-}$

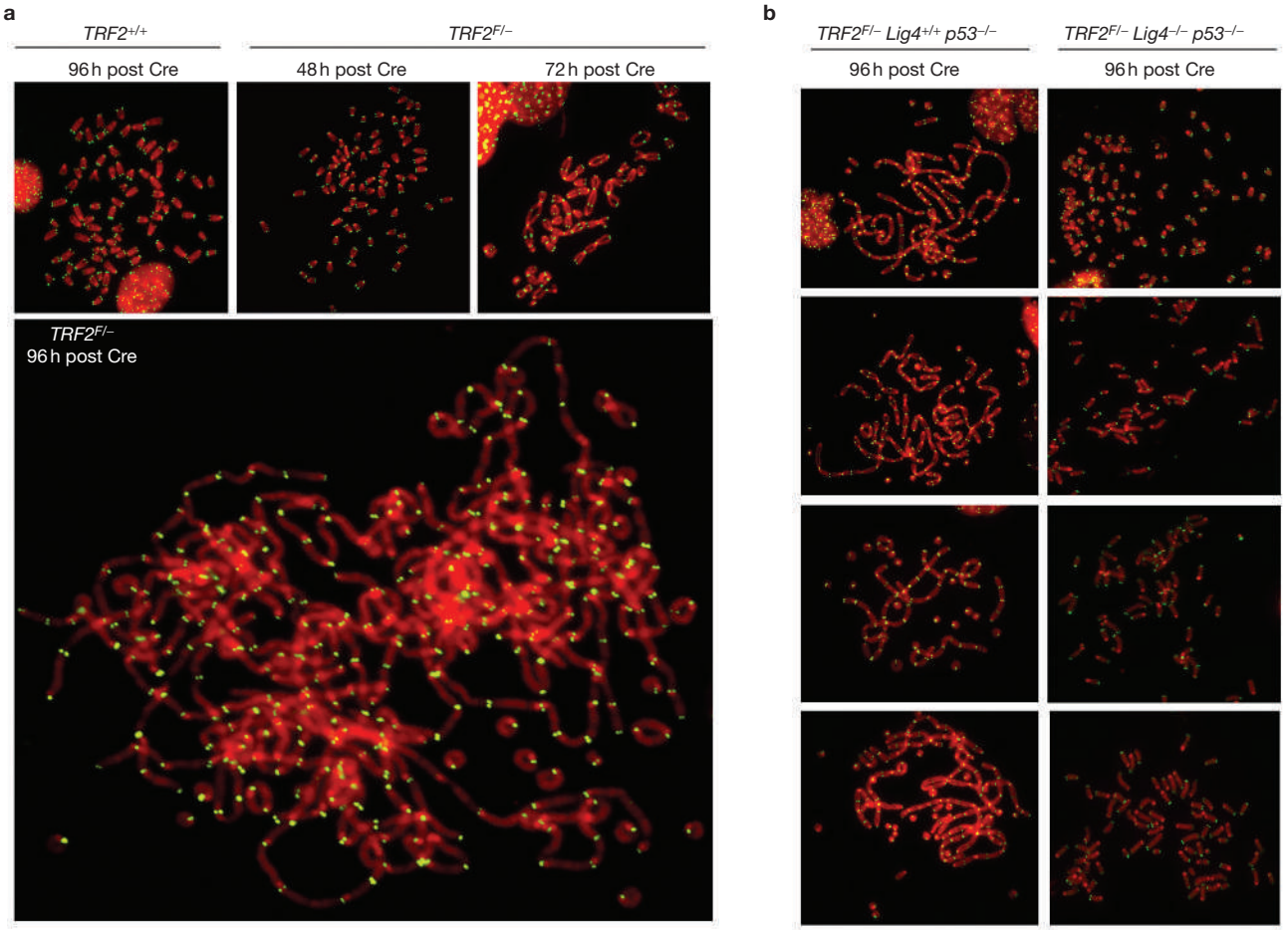

Figure 2 DNA ligase IV-mediated genome-wide telomere fusions upon *TRF2* deletion. (**a**) Metaphase spreads with telomeres detected by FISH. Cells derived from SV40LT-immortalized MEFs of the indicated genotypes were harvested at the indicated time points after introduction of Cre. (**b**) Telomeric FISH on metaphases from Lig4-proficient and -deficient *TRF2*$^{F/-}$ *p53*$^{-/-}$ MEFs that were harvested 96 h after introduction of Cre. Telomeric signals that were detected with a Tamra-labelled PNA $(TTAGGG)_3$ oligonucleotide are false coloured in green; DNA (DAPI) is false coloured in red.

cells (Fig. 3b; right panel and data not shown). The genomic blots also showed that the telomeric DNA was not degraded after TRF2 depletion even under conditions that block the repair of deprotected telomeres by NHEJ. The induction of telomere fusion upon inhibition of TRF2 function and their dependence on DNA ligase IV is consistent with previous experiments in which TRF2 was partially deactivated with a dominant-negative allele[6]. However, telomere fusions were ~50-fold more frequent in the *TRF2*-null cells, indicating that the dominant-negative *TRF2* is a relatively poor inhibitor of TRF2 function. Although *Lig4*$^{-/-}$ *p53*$^{-/-}$ cells did not form telomere fusions, their long-term survival was dependent on TRF2 (data not shown). The mechanism by which *TRF2*$^{-/-}$ *Lig4*$^{-/-}$ *p53*$^{-/-}$ cells arrest or die is currently under investigation.

The generation of a homogeneous population of cells, in which nearly all telomeres persisted in a free state without the protection of TRF2, provided the opportunity to correlate the structure of the chromosome ends with the cellular response. The status of the telomeric overhangs was assessed using an in-gel hybridization method that allows quantification of the single-stranded TTAGGG repeats. In this assay, a labelled CCCTAA probe is annealed to native DNA and the overhang signal is normalized to the total TTAGGG repeat signal obtained after in-gel denaturation of the DNA. After deletion of *TRF2* from NHEJ-proficient cells, most of the overhang signal disappeared rapidly (Fig. 3b and data not shown), as anticipated from previous studies with the dominant-negative allele of *TRF2* (refs 1, 6). Unexpectedly, when *TRF2* was deleted from *Lig4*$^{-/-}$ *p53*$^{-/-}$ cells, the overhang signal did not decrease; the normalized overhang signal after Cre introduction was slightly higher (119 ± 18% s.d.; $n = 3$) than the normalized overhang signal of untreated cells (set at 100%). Treatment with the 3′ end specific exonuclease I confirmed that the single-stranded TTAGGG repeats were at a 3′ end (Fig. 3b), and controls with a probe for the C-rich telomeric strand confirmed the specificity of the assay (data not shown). Degradation of the telomeric 3′ overhang upon TRF2 inhibition is known to require the nucleotide excision repair endonuclease ERCC1/XPF[18]. The lack of overhang degradation in *Lig4*$^{-/-}$ *p53*$^{-/-}$ cells indicates that the action of ERCC1/XPF at telomeres was coupled to the NHEJ machinery. ERCC1/XPF has not yet been implicated in global NHEJ but most NHEJ takes place in the context of short overhangs, and directed analysis of joining events at ends with long 3′ overhangs has not been performed. One possibility is that ERCC1/XPF is indeed generally involved in NHEJ of ends with extensive 3′ overhangs and that this nuclease is regulated by DNA-PKcs within the context of the NHEJ complex. This type of regulation by DNA-PK has been documented for another NHEJ nuclease, Artemis, which removes hairpins during V(D)J recombination[19].

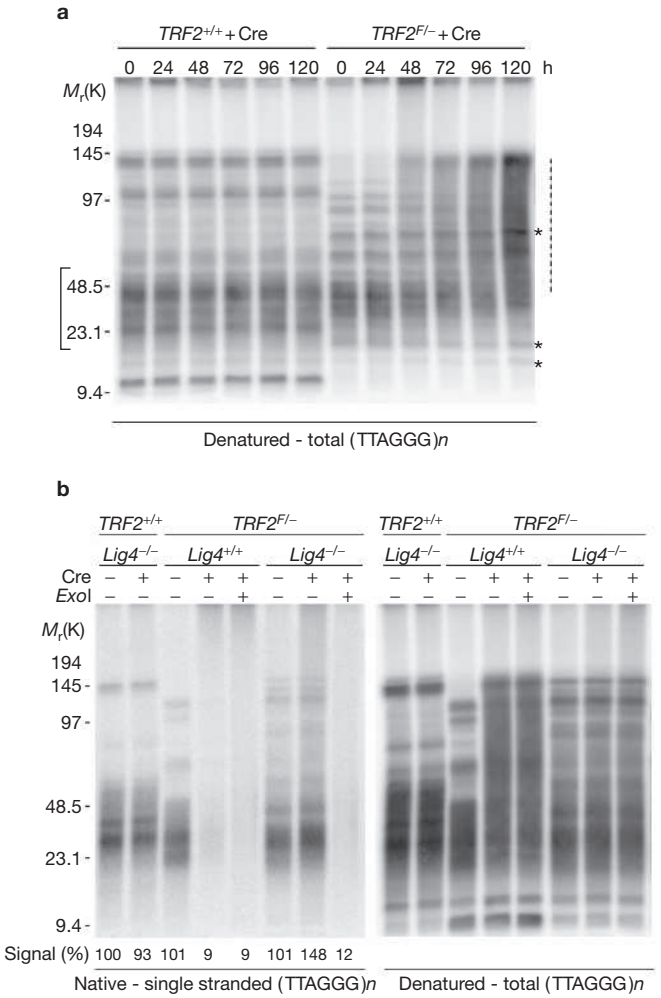

Figure 3 Lack of degradation of telomeric DNA in *TRF2*$^{-/-}$ *Lig4*$^{-/-}$ cells. (**a**) Time course of telomere fusions after deletion of *TRF2* detected by CHEF gel analysis of telomeric *Mbo*I fragments. Telomeric DNA was denatured in gel and hybridized with an end-labelled $(CCCTAA)_4$ probe. The asterisks indicate presumed chromosome internal sites with homology to the probe. The bracket on the left shows the position of most mouse telomeric fragments. The dotted line on the right of the gel indicates fused telomeres. Telomeric restriction patterns vary between individual mouse embryos (littermates). Cells were immortalized with SV40LT. (**b**) Telomeric overhang assay and corresponding telomeric DNA signal after *TRF2* deletion from *Lig4*$^{+/+}$ *p53*$^{-/-}$ and *Lig4*$^{-/-}$ *p53*$^{-/-}$ MEFs. Cells with the indicated genotypes were harvested at 96 h post Cre infection, embedded in agarose plugs, treated with *Exo*I (as indicated), and digested with *Mbo*I. Native DNA fractionated on a CHEF gel was hybridized *in situ* to a $(CCCTAA)_4$ probe to detect the G-strand overhang (left) and signals were quantified. The DNA was then denatured *in situ* and rehybridized to the same probe to detect all TTAGGG repeat DNA (right). Overhang signals in each lane were normalized to the total TTAGGG repeat signal and compared with control cells (set at 100%).

Because the telomeric DNA remained intact in *TRF2*$^{-/-}$ *Lig4*$^{-/-}$ *p53*$^{-/-}$ cells, this system presented an opportunity to determine whether overhang loss was required for the telomere damage response. The DNA damage response at chromosome ends can be monitored using the TIF (telomere dysfunction induced foci) assay[5], which monitors the association of 53BP1, γ-H2AX, and/or other DNA damage response factors with telomeres. In this assay, telomeres are detected with an antibody to TRF1, which remains on telomeres even when TRF2 is absent (Fig. 1c). As expected, deletion of *TRF2* resulted in the formation of γ-H2AX and 53BP1 foci that colocalized with TRF1 (Fig. 4a). By 96 h after introduction of Cre, ~50% of the *TRF2*$^{F/-}$ *p53*$^{-/-}$ cells contained at least four TIFs (see Supplementary Information, Table S2). Most of these cells contained 53BP1 on at least 20% of their telomeres (Fig. 4a; see Supplementary Information, Table S2 and data not shown), indicating a robust induction of the DNA damage response in this setting. Because TRF1 binds TTAGGG repeats at chromosome internal sites as well as at telomeres[20], the assay cannot distinguish between TIFs at genuine telomeres and DNA damage foci at telomeres that have become fused by NHEJ. However, the higher TIF index of NHEJ-deficient cells (see below) would argue that most TIFs in the *TRF2*$^{-/-}$ *p53*$^{-/-}$ cells represent deprotected telomeres prior to fusion. As expected from previous data, the DNA damage foci that formed upon TRF2 depletion also contained Nbs1, Mre11 and phosphorylated Rad17 (see Supplementary Information, Fig. S3). The TIFs were accompanied by phosphorylation of the ATM kinase on Ser 1981 and the ATM target Chk2 also became phosphorylated (Fig. 4c), in agreement with the idea that ATM is primarily responsible for telomere damage signalling[4,5,17,21]. Both phosphorylation events were specifically associated with *TRF2* deletion, appearing 48–72 h after Cre introduction into *TRF2*$^{F/-}$ but not *TRF2*$^{F/+}$ cells (data not shown).

Despite the retention of the telomeric overhang, *TRF2*$^{F/-}$ *Lig4*$^{-/-}$ *p53*$^{-/-}$ cells showed a robust induction of TIFs after deletion of *TRF2* (Fig. 4a, b, d). TIFs were observed in ~90% of the Cre-treated cells, and in these cells >80% of the telomeres were associated with 53BP1 (Fig. 4a, b and see Supplementary Information, Table S2). Immunofluorescence analysis indicated that 96 h after deletion of *TRF2*, approximately 75% of all telomeres in the cultures behaved as sites of DNA damage, even though no obvious loss of the telomeric DNA had occurred (see Supplementary Information, Table S2). In addition, *TRF2*$^{-/-}$ *Lig4*$^{-/-}$ *p53*$^{-/-}$ MEFs showed phosphorylation of ATM and Chk2 (Fig. 4d). The telomere damage response in *Lig4*$^{-/-}$ cells seemed to involve a larger fraction of the telomeres (75% versus 13% in *Lig4*$^{+/+}$ cells; see Supplementary Information, Table S2). This enhanced TIF response can be explained by the lack of 'repair' of deprotected telomeres in *Lig4*$^{-/-}$ cells, because TIFs are presumed to disappear once NHEJ has joined dysfunctional telomeres.

Collectively, the data show that deprotected telomeres, at least within the context of TRF2 loss, can be perceived as sites of DNA damage without detectable degradation of the telomeric DNA. In this regard, the mammalian telomere damage response may be different from the budding yeast response to dysfunctional telomeres, which involves extensive degradation of the telomeric 5′ strand. Our findings also argue that the suppression of the DNA damage response at mammalian telomeres requires more than simply the integrity of the telomeric DNA. What other aspect of the telomeres could prevent cells from perceiving the chromosome end as a DNA lesion? We can envisage two models. In the first, functional telomeres could contain a repressor of the DNA damage signal transduction pathway, thus actively blocking potential signalling. A candidate for such a repressor is TRF2, which is very abundant at telomeres and has the ability to block ATM kinase signalling in certain settings[22]. Since the amount of bound TRF2 correlates with telomere length[20], excessively shortened telomeres might be detected as sites of DNA damage because there is too little TRF2 to effectively block ATM. However, in the setting of telomere attrition, other signals may also be generated. A second model

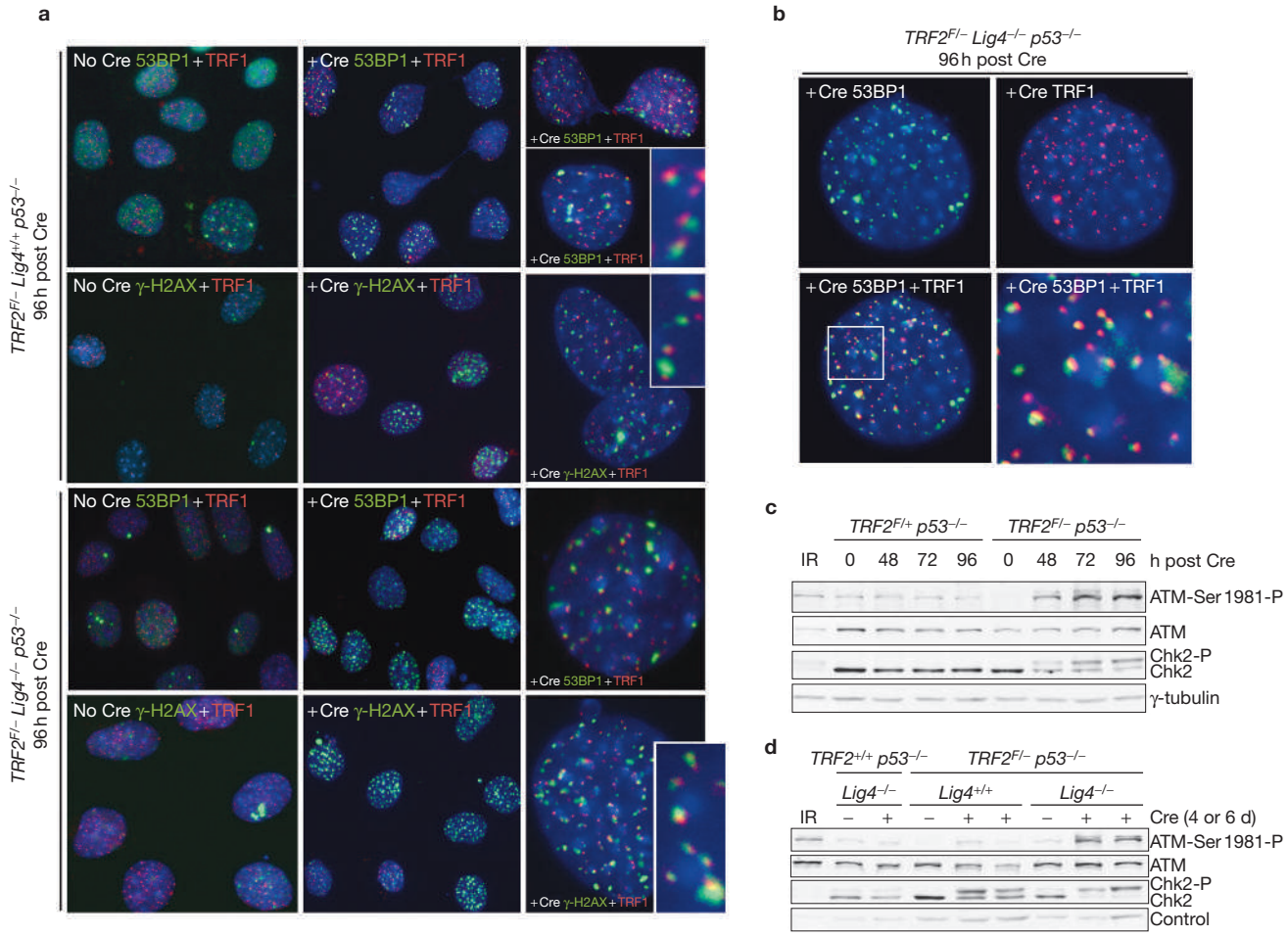

Figure 4 DNA damage response upon *TRF2* deletion from $TRF2^{F/-}$ $Lig4^{+/+}$ $p53^{-/-}$ and $TRF2^{F/-}$ $Lig4^{-/-}$ $p53^{-/-}$cells. (**a**, **b**) Immunofluorescence for TRF1 (TRITC; red), 53BP1 and γ-H2AX (each FITC; green) before and 96 h after introduction of Cre (as indicated). Enlarged images to the right in **a** show sites of DNA damage response at telomeres. In **b**, separate immunofluorescence signals for 53BP1 and TRF1 are shown. Bottom panels show the merged signal at two magnifications. DNA is stained blue (DAPI). (**c**, **d**) Immunoblots detecting phosphorylation status of ATM and Chk2 in MEFs of the indicated genotypes at indicated time points after introduction of Cre. Loading control in panel **d** is a band that cross-reacts with the Chk2 antibody. IR, γ-irradiation control. Cells were irradiated at 3 Gy; protein lysates were prepared 1 h post-irradiation.

posits that the t-loop structure[3] blocks the DNA damage response. One mechanism could involve telomeric nucleosomes. Vertebrate telomeres and t-loops are known to contain nucleosomes[23], but the modification state of core histones and the higher order nucleosomal organization have not been established. It is possible that t-loops, perhaps aided by telomeric proteins, enforce a nucleosomal organization that resembles the chromatin of intact chromosomal DNA, thus masking the chromosome ends from factors that detect DSBs based on altered chromatin state[9,24].

It has recently become clear that the mammalian telomere damage response strongly resembles, or is identical to, the canonical response to DSBs. Definition of the telomere damage signal may therefore be informative in the wider context of the DNA damage response elsewhere in the genome. The conditional TRF2 inactivation system allows for the controlled and synchronous induction of a DNA damage signal at ~100 molecularly marked sites — the ends of chromosomes — providing a unique opportunity to dissect the molecular nature of the signal. Because telomere damage can activate both the ATM kinase pathway and, in absence of ATM, the ATR pathway[25,26], this system could prove to be a versatile tool. □

METHODS

Gene targeting. The *Terf2* locus was isolated by screening a P1 129Sv library (Genome Systems, St Louis, MO) with a probe corresponding to the *TRFH* domain of mouse *TRF2*. A 10-kilobase *Hin*dIII fragment containing exons 1, 2 and 3 was used to build the targeting construct. A *Pst*I site upstream of exon 1 was replaced with *lox*P and *Hin*dIII sites; the second *lox*P site displaced the *Eco*RI site downstream of exon 2. The final targeting construct was generated by insertion of the modified locus into pGKneobpAlox2PGKDTA vector (a gift from T. Jacks, MIT, Cambridge, MA), which includes a PGK neo cassette flanked by the third *lox*P site and a negative selection (DTA) cassette. The vector was linearized with *Xho*I, and gene targeting was performed following standard techniques using the embryonic stem cell line E14 derived from 129P2/Ola. Embryonic stem cell clones containing the correct integration event were identified by genomic blotting. Cre recombinase was introduced transiently by electroporation of pCre-pac plasmid into appropriately targeted embryonic stem cell clones and selected for 48 h in 1 μg^{-1} ml^{-1} puromycin to obtain clones with either the fully deleted *TRF2* locus or clones with the conditional $TRF2^{F/+}$ allele. Embryonic stem cell clones were screened by genomic blot analysis of *Hin*dIII-digested DNA according to standard methods. Three embryonic stem cell clones for each allele were then used to generate chimaeras and subsequently lines of mice heterozygous or *F*/+ for TRF2. TRF2-targeted mice were maintained in a mixed 129/BL6 background. Intercrosses with $Lig4^{+/-}$ (ref. 27) and $p53^{-/-}$ (ref. 28) were performed to obtain *TRF2* conditional and null alleles in a $p53^{-/-}$ or in $Lig4^{-/-}$ $p53^{-/-}$ backgrounds. *Lig4*-targeted mice were maintained as heterozygotes.

Polymerase chain reaction (PCR) screening of *TRF2* genomic locus was performed using the following primers: P3A, 5′-CCAACCAGGGATACACAGTAG-3′; P2A2, 5′-GAGAGTTTGTTAAGTAGCTGCCAAG-3′; and P4A, 5′-ATCCGTAGTTCCTCTTGTGTCTG-3′. Primers P3A (140 bp 5′ to *Pst*I/*lox*P site) and P4A (88 bp 3′ of 5′ *lox*P site) amplify the wild-type and 'floxed' (flanked by *lox*P sites) alleles; P3A and P2A2 (211 bp 3′ of second *lox*P site) amplify the null allele. PCRs were performed for 35 cycles (at 94 °C for 40 s, 56 °C for 40 s, 72 °C for 1 min).

Conditional deletion of *TRF2* from MEFs. MEFs were isolated from E12.5–E13.5 embryos according to standard protocols. Briefly, after removal of the head and organs, tissue was minced and rinsed in ice-cold PBS, incubated in trypsin/EDTA (Gibco, Grand Island, NY) on ice for 2 h before dissociating in complete medium. Cells were resuspended in medium, and plated in 10-cm plates. After 48 h, confluent cultures were harvested and samples stored in liquid nitrogen (passage 1 MEFs). For continuous culturing, MEF cultures were split 1:3 or 1:4. Primary MEFs were grown in DMEM containing 10% fetal bovine serum, 100 U ml^{-1} penicillin, 0.1 μg ml^{-1} streptomycin, 0.2 mM L-glutamine, 0.1 mM non-essential amino acids, 1 mM sodium pyruvate and 50 μM β-mercaptoethanol. Immortalized MEFs were cultured in the same media but without addition of amino acids, pyruvate and β-mercaptoethanol. Retroviral stocks of pMMPHit&Run Cre-GFP[29], pLPC-Myc, pLPC-Myc-mTrf2, and pBabeSV40LT (a gift from G. Hannon) were generated using phoenix ecotropic cells as described[30]. For infections with hit-and-run (H&R) Cre retrovirus, 2–4 × 10^5 MEFs were incubated with viral supernatant supplemented with 4 μg ml^{-1} polybrene. After 10–12 h, the media was replaced with a second batch of viral supernatant and the cells were split 24 h later (1:4 or 1:6) and harvested at the indicated time points. For infection with pLPC-Myc and pLPC-Myc-mTrf2, cells were infected once for 24 h, then selected with 2 μg ml^{-1} puromycin for 3 days before infection with H&R Cre. To immortalize primary MEFs, early passage (P2) cells were infected with pBabeSV40LT and selected with 600 μg ml^{-1} G418 for 10–12 days.

Telomere fluorescence *in situ* hybridization (FISH). Cells were harvested at indicated time points and fixed as previously described[1]. Metaphase spreads were aged overnight, and peptide nucleic acid (PNA) FISH was performed as described[31] using a Tamra-$(TTAGGG)_3$ PNA probe (Applied Biosystems, Foster City, CA); DNA was counterstained with 4,6-diamidino-2-phenylindole (DAPI), and slides were mounted in 90% glycerol/10% PBS containing 1 μg ml^{-1} p-phenylene diamine (Sigma, St Louis, MO). Digital images were captured with a Zeiss (Thornwood, CA) Axioplan II microscope with a Hamamatsu (Bridgewater, MA) C4742-95 camera using Improvision (Lexington, MA) OpenLab software. Images were corrected for background and merged with Adobe Photoshop.

Pulse-field gel electrophoresis and in-gel detection of telomeric DNA. Clamped homogenous electric field (CHEF) gel electrophoresis of mouse DNA was performed essentially as described previously[32]. Cells were resuspended in PBS and mixed 1:1 (v/v) with 2% agarose (SeaKem LE agarose; Cambrex, Rockland, ME) to obtain 1 × 10^6 cells per agarose plug, digested with 1 mg ml^{-1} proteinase K in TENS buffer (100 mM EDTA, 0.2% sodium deoxycholate, 1% sodium lauryl sarcosine) and washed extensively in TE buffer (10 mM Tris pH 8, 1 mM EDTA). Plugs were incubated overnight at 37 °C with 60 U *Mbo*I in 0.5 ml. When *Exo*I digestion was performed on control for specificity of the single-strand G overhang signal, plugs were equilibrated in *Exo*I digestion buffer for 1 h, then incubated overnight with 1 U μl^{-1} *Exo*I at 37 °C. The next day, plugs were washed in TE, once in water, and digested with *Mbo*I as described above. Following digestion, plugs were washed in TE and equilibrated in 0.5 × TBE before loading into a 1% agarose-0.5 × TBE gel. The gel was run using CHEF-DRII PFGE apparatus (BioRad, Hercules, CA) in 0.5 × TBE for 24 h with the following settings: initial pulse, 5 min; final pulse, 5 min; 6 V cm^{-1} at 14 °C. In-gel hybridization with a ^{32}P-γATP end-labelled $(CCCTAA)_4$ oligonucleotide and subsequent denaturation and hybridization steps were performed as described[33]. Gels were exposed overnight onto a PhosphoImager screen, and single-stranded G overhang signal in each lane was quantified with ImageQuant software, and normalized to the total telomeric DNA signal obtained after denaturation. Ratios obtained after Cre treatment are given as a percentage of the control value obtained for the same cells not treated with Cre.

Immunofluorescence, immunoblotting and senescence-associated β-gal assay. Cells grown on coverslips were fixed in 2% paraformaldehyde, permeabilized in 0.5% NP-40, and incubated overnight at 4 °C with the following primary antibodies: affinity-purified rabbit peptide antibody against mTrf1, 644; affinity-purified rabbit antibodies raised against GST–mTrf2, 1254 and GST-mRap1, 1252; mouse monoclonal 53BP1 antibody (a gift from T. Halazonetis, Wistar Institute, Philadelphia, PA); γ-H2AX (Upstate Biotechnology, Lake Placid, NY); rabbit sera to Nbs1, 93-6' and Mre11, 42-7' (gifts from J. Petrini, MSKCC, New York, NY); phospho-Rad17 Ser 645 (Cell Signaling, Beverly, MA). Secondary antibodies raised against mouse and rabbit were labelled with Alexa 488 (Molecular Probes, Eugene, OR) and Rhodamine Red-X (RRX, Jackson, West Grove, PA), respectively. Cells were lysed in 2 × Laemmli buffer (100 mM Tris pH 6.8, 20% glycerol, 4% SDS, 5% β-mercaptoethanol, 0.05% bromophenol blue) at 10^4 cells per μl, denatured for 5 min at 100 °C, and sheared with a needle before loading the equivalent of 10^5 cells per lane on 7.5% SDS–PAGE. After immunoblotting, membranes were blocked in PBS with 10% milk and 0.1% Tween, and incubated overnight with primary antibodies in 1% milk: mTrf1; hTRF2, 647 (ref. 35); hRap1, 765 (ref. 36); phospho-ATM Ser 1981-P (Cell Signaling); phospho-Chk2 (BD Biosciences, San Jose, CA); ATM, MAT3 (gift); Myc, 9E10 (Oncogene/EMD Biosciences, San Diego, CA); γ-tubulin clone GTU 488 (Sigma). Blots were developed with enhanced chemiluminescence (Amersham, Piscataway, NJ). SA-β-gal staining was done as described[34] with staining overnight at 37 °C.

Note: Supplementary Information is available on the Nature Cell Biology website.

ACKNOWLEDGEMENTS

We gratefully acknowledge D. White for mouse husbandry and the RU Gene Targeting and Transgenic facilities for help in generating genetically modified mouse strains. F. Alt and C. Canyon are thanked for providing *Lig4*$^{-/-}$ mice, and T. Jacks for *p53*$^{-/-}$ mice. T. Halazonetis, J. Petrini, Y. Shiloh, T. Jacks, D. Livingston and G. Hannon are thanked for providing antibodies and plasmids. This work was supported by an NIH grant (GM49046-12) to T.d.L., and by funding from The Rockefeller University's Women & Science Fellowship Program, and by The Leukemia & Lymphoma Society to G.B.C.

COMPETING FINANCIAL INTERESTS

The authors declare that they have no competing financial interests.

Received 4 April 2005; accepted 27 May 2005
Published online at http://www.nature.com/naturecellbiology.

1. van Steensel, B., Smogorzewska, A. & de Lange, T. TRF2 protects human telomeres from end-to-end fusions. *Cell* **92,** 401–413 (1998).
2. Stewart, S. A. *et al.* Erosion of the telomeric single-strand overhang at replicative senescence. *Nature Genet.* **33,** 492–496 (2003).
3. Griffith, J. D. *et al.* Mammalian telomeres end in a large duplex loop. *Cell* **97,** 503–514 (1999).
4. d'Adda di Fagagna, F. *et al.* A DNA damage checkpoint response in telomere-initiated senescence. *Nature* **426,** 194–198 (2003).
5. Takai, H., Smogorzewska, A. & de Lange, T. DNA damage foci at dysfunctional telomeres. *Curr. Biol.* **13,** 1549–1556 (2003).
6. Smogorzewska, A., Karlseder, J., Holtgreve-Grez, H., Jauch, A. & de Lange, T. DNA ligase IV-dependent NHEJ of deprotected mammalian telomeres in G1 and G2. *Curr. Biol.* **12,** 1635–1644 (2002).
7. Garvik, B., Carson, M. & Hartwell, L. Single-stranded DNA arising at telomeres in cdc13 mutants may constitute a specific signal for the RAD9 checkpoint. *Mol. Cell. Biol.* **15,** 6128–6138 (1995).
8. Zou, L. & Elledge, S. J. Sensing DNA damage through ATRIP recognition of RPA-ssDNA complexes. *Science* **300,** 1542–1548 (2003).
9. Bakkenist, C. J. & Kastan, M. B. DNA damage activates ATM through intermolecular autophosphorylation and dimer dissociation. *Nature* **421,** 499–506 (2003).
10. Karlseder, J. *et al.* Targeted deletion reveals an essential function for the telomere length regulator Trf1. *Mol. Cell. Biol.* **23,** 6533–6541 (2003).
11. Chiang, Y. J., Kim, S. H., Tessarollo, L., Campisi, J. & Hodes, R. J. Telomere-associated protein TIN2 is essential for early embryonic development through a telomerase-independent pathway. *Mol. Cell. Biol.* **24,** 6631–6634 (2004).
12. Liu, D., O'Connor, M. S., Qin, J. & Songyang, Z. Telosome, a mammalian telomere-associated complex formed by multiple telomeric proteins. *J. Biol. Chem.* **279,** 51338–51342 (2004).
13. Ye, J. Z. *et al.* TIN2 binds TRF1 and TRF2 simultaneously and stabilizes the TRF2 complex on telomeres. *J. Biol. Chem.* **279,** 47264–47271 (2004).
14. Kim, S. H. *et al.* TIN2 mediates functions of TRF2 at human telomeres. *J. Biol. Chem.* **279,** 43799–43804 (2004).
15. Chin, L. *et al.* p53 deficiency rescues the adverse effects of telomere loss and cooperates with telomere dysfunction to accelerate carcinogenesis. *Cell* **97,** 527–538 (1999).
16. Smogorzewska, A. & de Lange, T. Different telomere damage signaling pathways in human and mouse cells. *EMBO J.* **21,** 4338–4348 (2002).

17. Karlseder, J., Broccoli, D., Dai, Y., Hardy, S. & de Lange, T. p53- and ATM-dependent apoptosis induced by telomeres lacking TRF2. *Science* **283,** 1321–1325 (1999).
18. Zhu, X. D. *et al.* ERCC1/XPF removes the 3′ overhang from uncapped telomeres and represses formation of telomeric DNA-containing double minute chromosomes. *Mol. Cell* **12,** 1489–1498 (2003).
19. Ma, Y., Pannicke, U., Schwarz, K. & Lieber, M. R. Hairpin opening and overhang processing by an Artemis/DNA-dependent protein kinase complex in nonhomologous end joining and V(D)J recombination. *Cell* **108,** 781–794 (2002).
20. Smogorzewska, A. *et al.* Control of human telomere length by TRF1 and TRF2. *Mol. Cell. Biol.* **20,** 1659–1668 (2000).
21. Bakkenist, C. J., Drissi, R., Wu, J., Kastan, M. B. & Dome, J. S. Disappearance of the telomere dysfunction-induced stress response in fully senescent cells. *Cancer Res.* **64,** 3748–3752 (2004).
22. Karlseder, J. *et al.* The telomeric protein TRF2 binds the ATM kinase and can inhibit the ATM-dependent DNA damage response. *PLoS Biol.* **2,** E240 (2004).
23. Makarov, V. L., Lejnine, S., Bedoyan, J. & Langmore, J. P. Nucleosomal organization of telomere-specific chromatin in rat. *Cell* **73,** 775–787 (1993).
24. Huyen, Y. *et al.* Methylated lysine 79 of histone H3 targets 53BP1 to DNA double-strand breaks. *Nature* **432,** 406–411 (2004).
25. Wong, K. K. *et al.* Telomere dysfunction and Atm deficiency compromises organ homeostasis and accelerates ageing. *Nature* **421,** 643–648 (2003).
26. Herbig, U., Jobling, W. A., Chen, B. P., Chen, D. J. & Sedivy, J. M. Telomere shortening triggers senescence of human cells through a pathway involving ATM, p53, and p21(CIP1), but not p16(INK4a). *Mol. Cell* **14,** 501–513 (2004).
27. Frank, K. M. *et al.* Late embryonic lethality and impaired V(D)J recombination in mice lacking DNA ligase IV. *Nature* **396,** 173–177 (1998).
28. Jacks, T. *et al.* Tumor spectrum analysis in p53-mutant mice. *Curr. Biol.* **4,** 1–7 (1994).
29. Silver, D. P. & Livingston, D. M. Self-excising retroviral vectors encoding the Cre recombinase overcome Cre-mediated cellular toxicity. *Mol. Cell* **8,** 233–243 (2001).
30. Jacobs, J. J. & de Lange, T. Significant role for p16(INK4a) in p53-independent telomere-directed senescence. *Curr. Biol.* **14,** 2302–2308 (2004).
31. Lansdorp, P. M. *et al.* Heterogeneity in telomere length of human chromosomes. *Hum. Mol. Genet.* **5,** 685–691 (1996).
32. Wang, R. C., Smogorzewska, A. & de Lange, T. Homologous recombination generates T-loop-sized deletions at human telomeres. *Cell* **119,** 355–368 (2004).
33. Karlseder, J., Smogorzewska, A. & de Lange, T. Senescence induced by altered telomere state, not telomere loss. *Science* **295,** 2446–2449 (2002).
34. Dimri, G. P. *et al.* A biomarker that identifies senescent human cells in culture and in aging skin *in vivo*. *Proc. Natl Acad. Sci. USA* **92,** 9363–9367 (1995).
35. Zhu, X. D., Kuster, B., Mann, M., Petrini, J. H. & de Lange, T. Cell-cycle-regulated association of RAD50/MRE11/NBS1 with TRF2 and human telomeres. *Nature Genet.* **25,** 347–352 (2000).
36. Li, B., Oestreich, S. & de Lange, T. Identification of human Rap1: implications for telomere evolution. *Cell* **101,** 471–483 (2000).

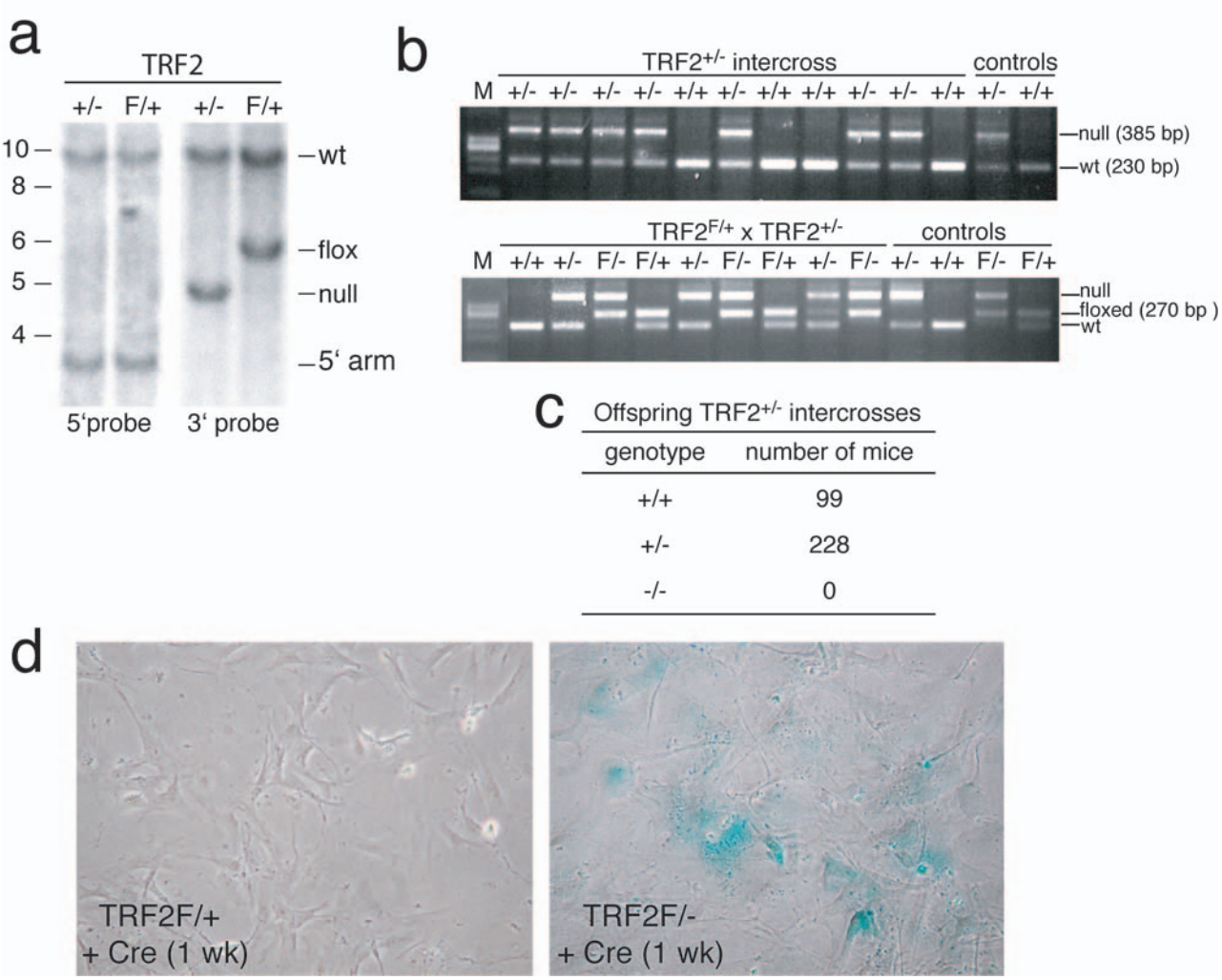

Figure S1 Deletion of TRF2 results in embryonic lethality and induction of senescences in MEFs. a, Southern blot analysis of genomic DNA isolated from positive ES clones post transient transfection with pCre-pac plasmid, digested with HindIII and hybridized to either the 5' or 3' probes. The fragments corresponding to the wt locus, conditional and null alleles are indicated, and molecular weight markers are in kb. b, PCR on offspring of intercrosses between TRF2+/- mice (top) and TRF2F/+ and TRF2 +/- mice. PCRs were done with P3A, P4A and P2A2 (see Fig. 1), and DNAs used as control were originally screened by Southern blot analysis. Sizes of the expected products are indicated. c, Number and genotype of offspring from TRF2+/- intercrosses. Expected number of -/- mice based on Mendelian inheritance ratio 1:2:1 is 81. d, Deletion of TRF2 in primary MEFs causes senescence. β-galactosidase staining of TRF2F/+ and TRF2F/- MEFs one week post infection with H&R Cre retrovirus.

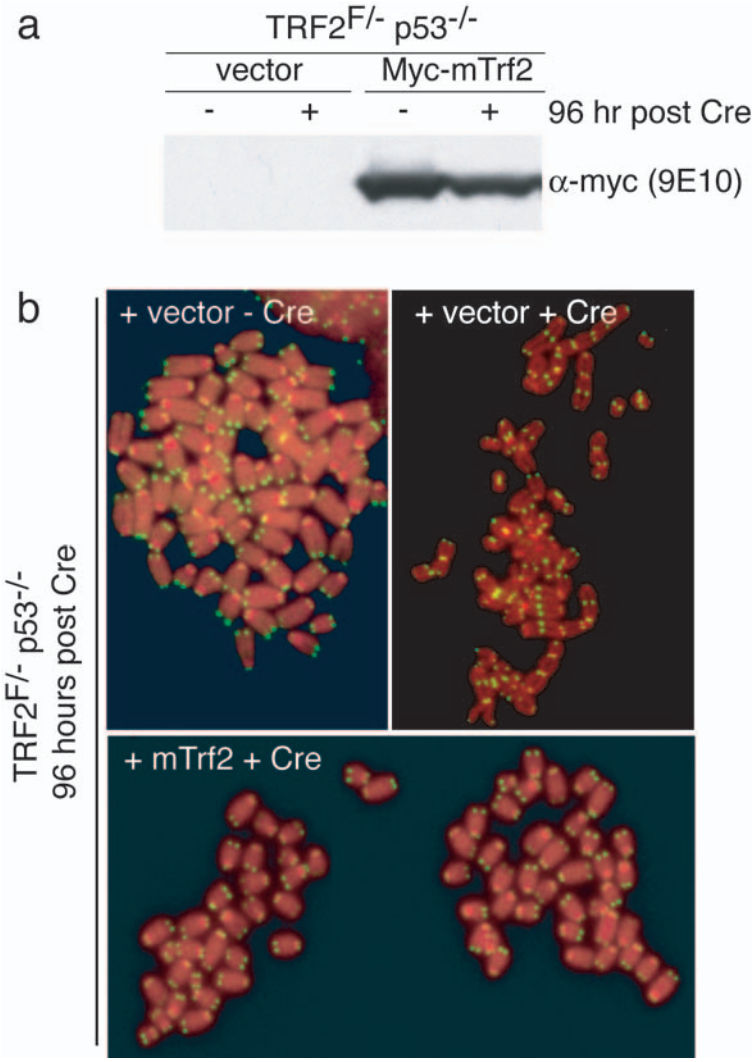

Figure S2 Exogenous TRF2 represses telomere fusions after TRF2 deletion from TRF2F/- p53-/- MEFs. Vector control (pLPC) or pLPCMyc-mTrf2 infected cells untreated were harvested 96 hours post Cre, and either (a) lysed in Laemmli buffer and analysed by immunolot with anti-Myc, or (b) fixed in methanol:acetic acid and spread on glass slides for telomeric FISH on metaphase spreads.

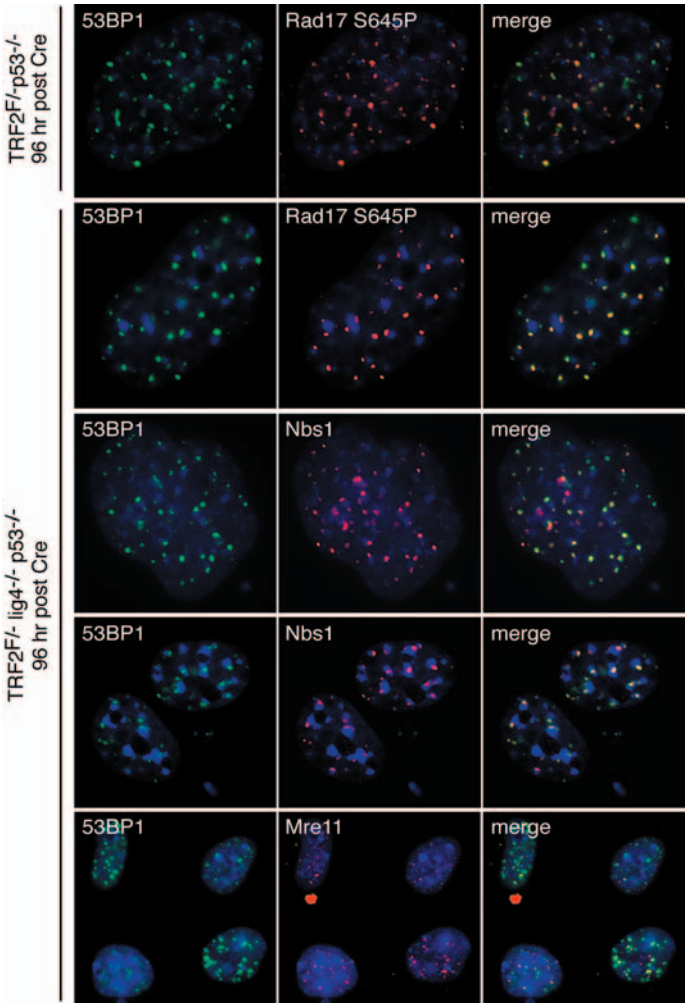

Figure S3 Phosphorylated Rad17, Nbs1 and Mre11 are at TIFs formed after TRF2 deletion. IF costaining for 53BP1 with either phosphoRad17, Nbs1 and Mre11 in the indicated MEFs at 96 hours post infection with H&R Cre retrovirus. Rabbit sera against phosphoRad17S645; Nbs1, 93-6'; and Mre11, 42-7' were detected with a RRX-conjugated seconary antibody; 53BP1 was detected with Alexa488 anti-mouse secondary antibody.

Table S1 Dependence of telomere–telomere fusions on DNA ligase IV

Genotype (all 53-/-)	Cre	Number of metaphases	% metaphases with >2 fusions	Fusions per metaphase
TRF2+/-lig4-/-	-	69	<3	<0.1
TRF2+/-lig4-/-	+	70	7	<0.1
TRF2F/-lig4+/+	-	63	<3	<0.1
TRF2F/-lig4+/+	+	81	100	61
TRF2F/-lig4-/-	-	59	<3	<0.1
TRF2F/-lig4-/-	+	109	17	0.5

Cells with the specified genotype were treated with Cre as indicated and metaphases processed for telomeric FISH. The incidence of chromosome end fusions with telomeric signals was noted on the indicated number of metaphases. Tabulated data was compiled from three independent infections with H&R Cre. All MEFs were p53 null.

Table S2 TIFs at most chromosome ends in DNA ligase IV-deficient cells lacking TRF2[a]

Genotype (all p53-/-)	Cre	Fraction of cells with ≥ 4 TIF (n)			Fraction of telomeres with 53BP1[b] in TIF+ nuclei	Estimated fraction of telomeres containing 53BP1[c]
		Experiment I	Experiment II	Experiment III		
TRF2+/-lig4-/-	-	14% (78)	6% (84)	12% (69)	12 % (359)	1%
TRF2+/-lig4-/-	+	11% (81)	4% (73)	6% (68)	13% (172)	<1%
TRF2F/-lig4+/+	-	8% (85)	4% (88)	5% (62)	9% (532)	<1%
TRF2F/-lig4+/+	+	56% (71)	45% (116)	67% (92)	23%(1304)	13%
TRF2F/-lig4-/-	-	11% (87)	2% (105)	8% (36)	11% (492)	<1%
TRF2F/-lig4-/-	+	86 % (85)	93% (109)	94% (51)	82%(1173)	75%

[a] MEFs with the indicated genotype were treated with Cre and processed for IF after 4 days. Telomere dysfunction Induced Foci (TIF) were detected based on co-localization of 53BP1 and TRF1 signals. All MEF were $p53^{-/-}$. [b] Data derived from experiment III. Nuclei with ≥4 TIF were examined for percentage of TRF1 loci that contained 53BP1. Number of telomeres examined is given in parenthesis. [c] Fraction of all telomeres in the cultures containing 53BP1 was estimated as average fraction of cells with ≥ 4 TIFs multiplied by the fraction of telomeres containing 53BP1 in TIF positive nuclei.